Published in final edited form as:
Nano Lett. 2011 March 9; 11(3): 1395–1400. doi:10.1021/nl200494t.

Magnetically-triggered Nanocomposite Membranes: a Versatile Platform for Triggered Drug Release

Todd Hoare[1,†], **Brian P. Timko**[2,3,†], **Jesus Santamaria**[4,5], **Gerardo F. Goya**[5], **Silvia Irusta**[4,5], **Samantha Lau**[3], **Cristina F. Stefanescu**[2], **Debora Lin**[3], **Robert Langer**[3], and **Daniel S. Kohane**[2,*]

[1]Department of Chemical Engineering, McMaster University, 1280 Main St. W, Hamilton, Ontario, Canada L8S 4L7

[2]Laboratory for Biomaterials and Drug Delivery, Department of Anaesthesiology, Division of Critical Care Medicine, Children's Hospital Boston, Harvard Medical School, 300 Longwood Ave., Boston, MA, U.S.A. 02115

[3]Department of Chemical Engineering, Massachusetts Institute of Technology, 45 Carleton St., Cambridge, MA, U.S.A. 02142

[4]Networking Biomedical Research Center of Bioengineering, Biomaterials and Nanomedicine (CIBERBBN). Maria de Luna, 11. Zaragoza 50018 Spain

[5]Institute of Nanoscience of Aragón, University of Zaragoza, Mariano Esquillor s/n 50018 Zaragoza, Spain

Abstract

Drug delivery devices based on nanocomposite membranes containing thermoresponsive nanogels and superparamagnetic nanoparticles have been demonstrated to provide reversible, on-off drug release upon application (and removal) of an oscillating magnetic field. We show that the dose of drug delivered across the membrane can be tuned by engineering the phase transition temperature of the nanogel, the loading density of nanogels in the membrane, and the membrane thickness, allowing for on-state delivery of model drugs over at least two orders of magnitude (0.1–10 μg/hr). The zero-order kinetics of drug release across the membranes permit drug doses from a specific device to be tuned according to the duration of the magnetic field. Drugs over a broad range of molecular weights (500–40,000 Da) can be delivered by the same membrane device. Membrane-to-membrane and cycle-to-cycle reproducibility is demonstrated, suggesting the general utility of these membranes for drug delivery.

Keywords

Iron oxide; nanogel; nanoparticles; triggered drug release; on-demand; superparamagnetism

Sustained drug release technology has been applied in a wide variety of medical fields1. Many devices are passive, exhibiting release kinetics that are either constant or decreasing over time. However, drug delivery devices that can be repeatedly switched on and off would be optimal for effective treatment of conditions such as diabetes, chronic pain, or cancer.[2]

*To whom correspondence should be addressed. Daniel.Kohane@childrens.harvard.edu.
†These authors contributed equally to this report.

Supporting Information Available: Methods and Supporting Figures. This material is available free of charge via the Internet at http://pubs.acs.org.

To this end, environmentally responsive ("smart") materials have been developed that can respond to stimuli that are either internal to the patient (e.g. body temperature) or external (e.g. a remotely-applied magnetic field). Temperature-sensitive drug delivery devices have been developed based on the thermoreversible polymer poly(N-isopropylacrylamide) (PNIPAm)[3], which has been incorporated into implantable hydrogels4–9, microparticles10, nanoparticles[11–14], and surface-grafted polymers[15–27]. Examples of magnetically-activated materials include superparamagnetic nanoparticles, which absorb power when placed in an oscillating magnetic field and transfer heat to the surrounding medium. These nanoparticles have been used to achieve drug release from polymer scaffolds[28], sheets[29], liposomes[30], microspheres[31, 32], microcapsules[33], and nanospheres[34–36], typically by mechanical disruption of the drug-biomaterial matrix. However, the quantity of drug contained by most of these "smart" carriers is relatively small, and drug release is often characterized either by a single burst event or inconsistent dosing as a function of triggering cycle.

To achieve both triggered drug release and consistent dosing, we previously reported composite membranes containing both temperature-sensitive polymer nanoparticles (nanogel) and magnetically activated superparamagnetic nanoparticles[37]. These composite membranes were used to contain reservoirs of drug and achieved repeatable, on demand, on-off switching of molecular flux upon application of an oscillating magnetic field. However, in order to successfully translate this technology to the clinic, factors affecting the on-state release rate, on/off ratio, and drug-membrane interactions need to be understood, and rationally controlled.

In the present study, we report, for the first time, the relation between the chemical and physical composition of the membranes and the release kinetics of several model compounds. Specifically, we demonstrate (a) how the critical on-off temperature of the device can be controlled by the chemical composition of the polymer nanogel, (b) how drug release can be tuned as a function of membrane thickness and nanogel loading density, and (c) how these membranes can be used to deliver both small and large, and anionic and cationic molecules.

Membranes were produced by suspending or dissolving superparamagnetic iron oxide nanoparticles, PNIPAm-based nanogels (NGs), and ethyl cellulose (the membrane matrix material) in ethanol and evaporating to form a film (Figure 1A–C; see Supporting Information for Methods). We have hypothesized that the nanogel forms a disordered, interconnected network througout the matrix. The superparamagnetic nanoparticles behave as local heat sources that are activated (turned on) by an external, oscillating magnetic field.[38] Temperature-triggered collapse of the PNIPAm enables transport of material (i.e. drug molecules from an enclosed reservoir) across the membrane (Figure 1D).

We produced membranes containing various types and quantities of nanogels prepared to exhibit different phase transition temperatures (see Supporting Information for Methods). The phase transition temperature was controlled by copolymerizing NIPAm with N-isopropylmethacrylamide (NIPMAm) and acrylamide (AAm) (Table 1). Figure 2A indicates that copolymerization of different combinations of precursors can shift the transition temperature of the nanogels from ~32°C (NG-32) to ~46°C (NG-46). Of particular note, using this copolymerization approach, the transition temperature can be shifted without inducing a change in the total percentage volume change observed upon nanogel deswelling (Table 2, $p>0.2$ for all pair-wise comparisons). As a result, highly thermoresponsive nanogels can be synthesized that have a range of phase transition temperatures appropriate for a variety of different triggering applications.

The transition temperature of molecular flux through a membrane correlates well with the phase transititon temperature of its consitutent nanogels, as shown in Figure 2B. However, these data also indicate a temperature offset between flux and transition temperature. For example, in the case of the NG-32 membrane at 30°C, the nanogel shrank (See Methods in Supporting Information) by ~250 nm without the occurrence of a significant change in permeability. A similar trend is observed with the NG-37 membrane, with a ~200 nm size decrease required prior to a significant increase in membrane permeability. This lag may be attributable to the presence of a disordered pore network inside the membranes; small volume changes in the nanogel presumably cannot generate sufficient free volume over the full thickness of the membrane to significantly change permeability of the membrane.

To change the flux of drug through the membrane in the on state, the permeability of the membrane must be controlled and optimized. Tuning the membrane thickness is one straightforward approach. Increasing the membrane thickness increased the diffusional path length of a drug molecule through the membrane and thus reduced the rate of drug release (Figure 3). The thinnest membrane tested (90 ± 14 μm thick) released 6.4 ± 0.4 μg/hr sodium fluorescein while the thickest membrane tested (288 ± 32 μm thick) released only 0.4 ± 0.1 μg/hr sodium fluorescein. Mass transfer rate correlated with membrane thickness measured with calipers. A trade-off existed between membrane strength and membrane flux; thicker membranes that are presumably stronger release drug more slowly. Drug release rate could be further tuned by adjusting the concentration gradient of drug across the membrane, as a linear correlation exists between the initial drug concentration and the membrane flux (Supporting Figure S1).

The permeability of the membrane can also be tuned by adjusting the density of nanogel particles embedded within. Increasing the nanogel content increased the number of thermoresponsive pores templated into the membrane and thus increased the total free volume generated inside the membrane when the nanogels underwent a phase transition, leading to significant increases in drug flux through the membrane (Figure 4). We found that at nanogel loadings of 25wt% or less, a logarithmic relationship existed between membrane flux and nanogel loading (Figure 4B, $R^2 > 0.99$). As a result, the mass flux of sodium fluorescein through the membrane could be tuned over at least two orders of magnitude (0.1–10 μg/hr) by changing the nanogel content inside the membrane. The same trend was observed when an oscillating magnetic field was used as the on-off trigger (Figure 5); the membrane containing 23 wt% nanogel exhibited a lower average drug release rate in the on state (4.1 μg/min) than did the 28 wt% nanogel membrane (5.7 μg/min). In this case, both membranes were heated by the same ~2.2°C temperature gradient under the applied oscillating magnetic field, due to the identical ferrofluid content in each membrane.

However, the ratio between the flux in the on state and the off state (i.e. the flux selectivity between the on and off states) decreased as the amount of nanogel in the membrane increased, particularly at higher nanogel loadings. For the data presented in Figure 4, the ratio between sodium fluorescein flux at 45 °C (on) and 37 °C (off) was 15.2 ± 2.6 for a membrane containing 12 wt% nanogel, 8.1 ± 1.5 for a membrane containing 25 wt% nanogel, and 6.0 ± 0.5 for a membrane containing 32 wt% nanogel. Thus, while increasing the nanogel concentration consistently increased the drug flux through the membrane, increased flux was accompanied by decreased on-off ratio. Furthermore, membranes prepared with 37 wt% nanogel exhibited high flux in both the on and off states regardless of temperature, representing a “leaky” system that would be less useful for on-demand drug delivery (data not shown).

At all different membrane thicknesses and for all nanogels tested, drug release occurred with zeroorder release kinetics over at least 24 hours ($R^2 > 0.98$ in all cases in Figures 3 and 4) in

the on state. Therefore, the total dose of drug delivered over time could be dynamically adjusted by varying the duration of the oscillating magnetic field. Zero-order release was also observed in the off state, although the rate of drug release was significantly reduced (Supporting Figure S2). While the nanogel loading and/or membrane thickness could be engineered to control the magnitude of the drug release rate targeted for a particular membrane device, the duration of the on/off states of the magnetic field can be easily controlled by the duty cycle of the power source, thus controlling the total amount of drug delivered using any specific device and providing full on-demand control (at both the design stage and in the patient use stage) over drug delivery.

On-demand, zero order release was also achieved for the flux of drugs with a range of physical properties. Triggered release was demonstrated from a saturated solution of a 40 kDa molecular weight fluorescein-labelled dextran (Figure 6). Effective on-off switching of macromolecule release was observed, with 0.28 ± 0.08 μg/hr drug flux measured through the membrane in the on state and a flux ratio of 6.7 ± 1.2 between the on and off states. In comparison, sodium fluorescein release through the same membrane occured at a rate of 8.0 ± 2.8 μg/hr, but at a much lower concentration gradient (1.25 mg/mL, see Supporting Information for Methods), with a flux ratio of 8.0 ± 1.5 between the on and off states (see Figure 4). The lower permeability of the membrane to FITC-dextran was likely due to its higher molecular weight, and lower diffusion coefficient. On the other hand, the similar flux ratio observed between the large and small molecules suggests that the flux ratio was predominantly governed by the inherent properties of the membrane (e.g. nanogel loading and thickness).

Thermally-triggered drug release was also demonstrated for bupivacaine, a small molecule amphiphilic drug that is largely cationic at physiological pH (Supporting Figure S3). Thus, it was possible to deliver drugs with different molecular weights and different charges using the same membrane-based delivery vehicles.

Successful use of these membranes as long-term, on-demand drug delivery vehicles requires high reproducibility of cycle-to-cycle and device-to-device drug release. A representative example of four replicate runs for the 25 wt% NG-37 membrane is shown in Supporting Figure S4. For a single membrane, the cycle-to-cycle variability is low; indeed, there is no statistical difference in drug release in either the on or off states on a cycle-to-cycle basis for any membranes tested in this work ($p > 0.07$ for any pair-wise comparison over four on-off cycles). Thus, a single membrane gives highly reproducible release profiles upon multiple triggering events. Similar results were observed over 10 triggering cycles when the membranes were fabricated into implantable reservoir drug delivery devices, although a slight lag in release was observed in the first on cycle, likely due to the need to first saturate the microgel-filled pores of the membrane with the drug prior to drug release. (Supporting Figure S5)

Membrane-to-membrane variability was low for the highly nanogel-loaded membranes ($p > 0.18$ for any pair-wise comparison between 32 wt% nanogel-functionalized membranes, Figure 4A) but increased for membranes with lower nanogel loadings ($p < 0.05$ for at least one pair-wise comparison of on state releases for all membranes prepared with nanogel loadings of 25wt% or less, Figures 4A and S5). Observed membrane-to-membrane variability was likely attributable to subtle differences in hand-mixing of the highly viscous precursor solution/suspension between different membranes, leading to slightly different nanogel distributions in replicate membranes. Automation of the mixing procedure could minimize this variability.

The composite membrane-based drug delivery devices described here offer a significant improvement over existing technologies since they can be readily engineered to achieve rational control over drug release kinetics for a variety of compounds. Our data show that it is possible to precisely control drug dosing over multiple orders of magnitude of dosings based on both the physical properties and compositions of the membrane and the duration of the on pulse applied to a given membrane. The frequency and power of the applied magnetic field could also be tuned to effect changes in drug dosing by changing the steady-state temperature of the device. Furthermore, our devices exhibit excellent reproducibility device-to-device as well as cycle-to-cycle. This tunability and reproducibility would present multiple options to the engineer, clinician, and patient for dynamically changing the specific level of basal drug release as well as on-demand drug dosing. Devices with performance metrics like the one presented here have the potential to be effective in vivo. Cellular and tissue reaction to the base components and the composite are benign.[37] As with all drug delivery systems, it will be important to demonstrate this anew with each drug payload, which could have a marked effect on biocompatibility.[39]

Supplementary Material

Refer to Web version on PubMed Central for supplementary material.

Acknowledgments

This research was funded by NIH grant GM073626 to DSK. TH acknowledges post-doctoral funding from the Natural Sciences and Engineering Research Council of Canada. BPT acknowledges a Ruth L. Kirschstein NRSA fellowship, NIH Award Number F32GM096546. SI and GFG acknowledge support from the Spanish MEC through the Ramon y Cajal program.

References

1. Chasin, M.; Langer, RS. Biodegradable polymers as drug delivery systems. Dekker, M., editor. New York: 1990. p. viii347
2. Timko BP, Dvir T, Kohane DS. Adv. Mater. 2010; 22(44):4925–4943. [PubMed: 20818618]
3. West JL. Nature Materials. 2003; 2(11):709–710.
4. Alexander C. Nature Materials. 2008; 7(10):767–768.
5. Ehrick JD, Deo SK, Browning TW, Bachas LG, Madou MJ, Daunert S. Nature Materials. 2005; 4(4):298–302.
6. Ehrbar M, Schoenmakers R, Christen EH, Fussenegger M, Weber W. Nature Materials. 2008; 7(10): 800–804.
7. Kikuchi A, Okano T. Advanced Drug Delivery Reviews. 2002; 54(1):53–77. [PubMed: 11755706]
8. Okuyama Y, Yoshida R, Sakai K, Okano T, Sakurai Y. Journal of Biomaterials Science-Polymer Edition. 1993; 4(5):545–556. [PubMed: 8241069]
9. Qiu Y, Park K. Advanced Drug Delivery Reviews. 2001; 53(3):321–339. [PubMed: 11744175]
10. Ichikawa H, Fukumori Y. Journal of Controlled Release. 2000; 63(1–2):107–119. [PubMed: 10640584]
11. Sahiner N, Alb AM, Graves R, Mandal T, McPherson GL, Reed WF, John VT. Polymer. 2007; 48(3):704–711.
12. Eichenbaum GM, Kiser PF, Dobrynin AV, Simon SA, Needham D. Macromolecules. 1999; 32(15):4867–4878.
13. Hoare T, Pelton R. Langmuir. 2008; 24(3):1005–1012. [PubMed: 18179266]
14. Snowden MJ. Journal of the Chemical Society-Chemical Communications. 1992; (11):803–804.
15. Alem H, Duwez AS, Lussis P, Lipnik P, Jonas AM, Demoustier-Champagne S. Journal of Membrane Science. 2008; 308(1–2):75–86.

16. Fu Q, Rao GVR, Ward TL, Lu YF, Lopez GP. Langmuir. 2007; 23(1):170–174. [PubMed: 17190500]
17. Okahata Y, Noguchi H, Seki T. Macromolecules. 1986; 19(2):493–494.
18. Yoshida M, Asano M, Safranj A, Omichi H, Spohr R, Vetter J, Katakai R. Macromolecules. 1996; 29(27):8987–8989.
19. Yoshida R, Kaneko Y, Sakai K, Okano T, Sakurai Y, Bae YH, Kim SW. Journal of Controlled Release. 1994; 32(1):97–102.
20. Choi YJ, Yamaguchi T, Nakao S. Industrial & Engineering Chemistry Research. 2000; 39(7): 2491–2495.
21. Hesampour M, Huuhilo T, Makinen K, Manttari M, Nystrom M. Journal of Membrane Science. 2008; 310(1–2):85–92.
22. Lee YM, Shim JK. Polymer. 1997; 38(5):1227–1232.
23. Liang L, Feng XD, Peurrung L, Viswanathan V. Journal of Membrane Science. 1999; 162(1–2): 235–246.
24. Akerman S, Viinikka P, Svarfvar B, Putkonen K, Jarvinen K, Kontturi K, Nasman J, Urtti A, Paronen P. International Journal of Pharmaceutics. 1998; 164(1–2):29–36.
25. Iwata H, Oodate M, Uyama Y, Amemiya H, Ikada Y. Journal of Membrane Science. 1991; 55(1–2):119–130.
26. Wang WY, Chen L. Journal of Applied Polymer Science. 2007; 104(3):1482–1486.
27. Wang WY, Chen L, Yu X. Journal of Applied Polymer Science. 2006; 101(2):833–837.
28. Zhao X, Kim J, Cezar CA, Huebsch N, Lee K, Bouhadir K, Mooney DJ. Proceedings of the National Academy of Sciences USA. 2011; 108(1):67–72.
29. Edelman ER, Kost J, Bobeck H, Langer R. Journal of Biomedical Materials Research. 1985; 19(1): 67–83. [PubMed: 4077873]
30. Muller-Schulte, D. Thermosensitive, biocompatible polymer carriers with changeable physical structure for therapy, diagnostics, and analytics. United States Patent Application. 10/578024. 2007.
31. Muller-Schulte D, Schmitz-Rode T. Journal of Magnetism and Magnetic Materials. 2006; 302(1): 267–271.
32. Zhang J, Misra RDK. Acta Biomaterialia. 2007; 3(6):838–850. [PubMed: 17638599]
33. Hu SH, Tsai CH, Liao CF, Liu DM, Chen SY. Langmuir. 2008; 24(20):11811–11818. [PubMed: 18808160]
34. Hu SH, Chen SY, Liu DM, Hsiao CS. Advanced Materials. 2008; 20(14):2690–2695.
35. Hu SH, Liu TY, Huang HY, Liu DM, Chen SY. Langmuir. 2008; 24(1):239–244. [PubMed: 18052081]
36. Liu TY, Hu SH, Liu DM, Chen SY, Chen IW. Nano Today. 2009; 4(1):52–65.
37. Hoare T, Santamaria J, Goya GF, Irusta S, Lin D, Lau S, Padera R, Langer R, Kohane DS. Nano Letters. 2009; 9(10):3651–3657. [PubMed: 19736912]
38. Jeong U, Teng XW, Wang Y, Yang H, Xia YN. Advanced Materials. 2007; 19(1):33–60.
39. Kohane DS, Langer R. Chemical Science. 2010; 1(4):441–446.

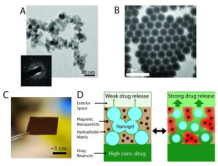

Figure 1. Overview of membrane composition and function

(A) TEM of superparamagnetic iron oxide nanoparticles. Inset: Diffraction pattern suggests an ensemble of randomly-oriented crystalline particles. (B) TEM image of dehydrated nanogel particles. (C) Photograph of membrane containing ferromagnetic nanoparticles and nanogel, distributed throughout an ethyclellulose matrix. (D) Proposed schematic of a cross-section of the membrane, showing nanogel particles (blue), iron oxide nanoparticles (dark brown), and ethylcellulose matrix (light brown). Upon application of a magnetic field, the magnetic nanoparticles release heat (red) and reversibly shrink the nanogel, enabling release of a drug (green) from a reservoir contained by the membrane.

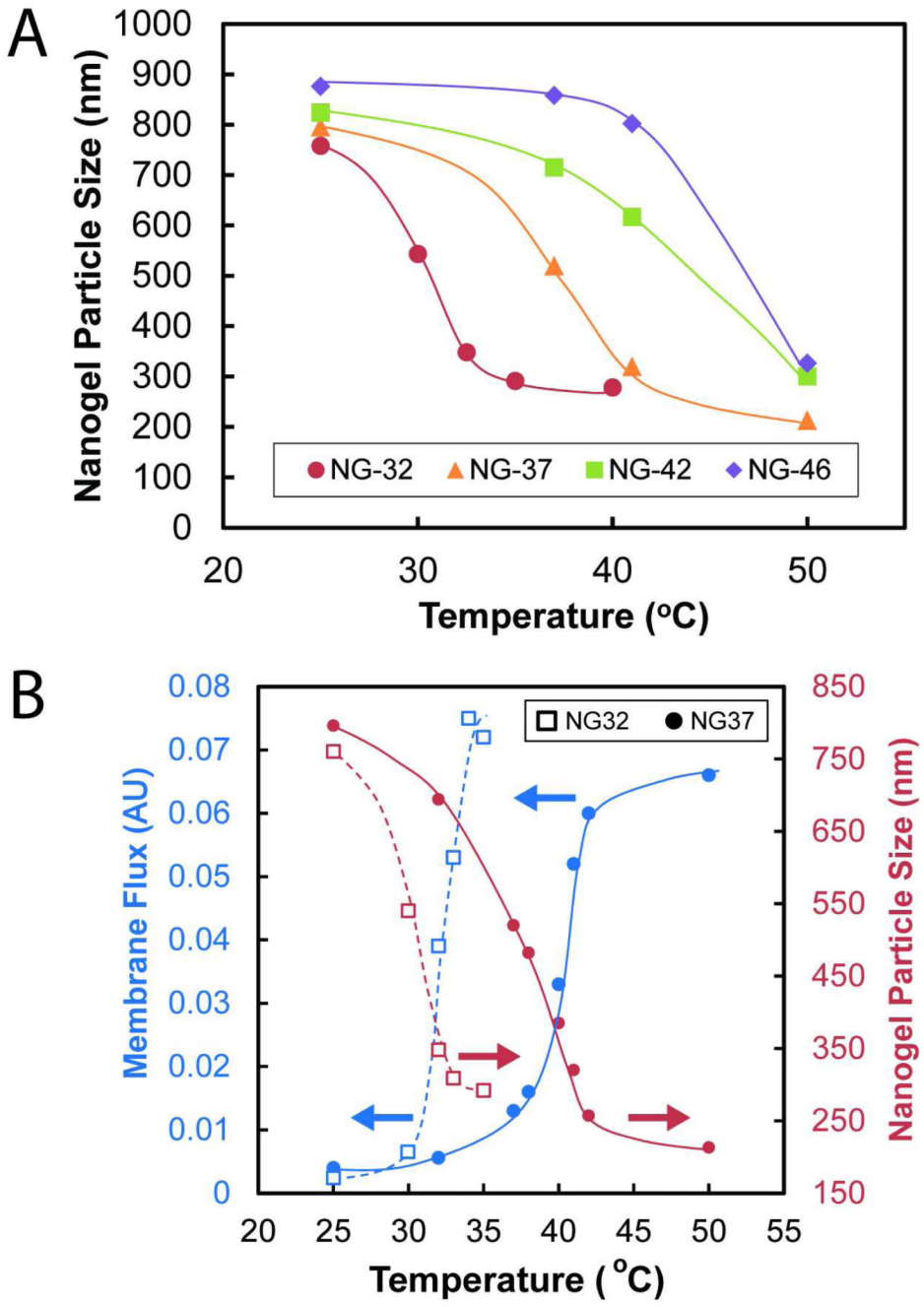

Figure 2. Membrane on-off temperature can be tuned by nanogel composition

(A) Volume phase transition behavior of four nanogel formulations containing differing amounts of NIPAm, NIPMAm, and AAm (see Table 1). (B) Correlation between nanogel particle size in suspension (red points / right axis) and the mass flux (blue points / left axis) of sodium fluorescein through membranes as a function of temperature, for membranes containing 25 wt% NG-32 (□) and NG-37 (●) nanogels.

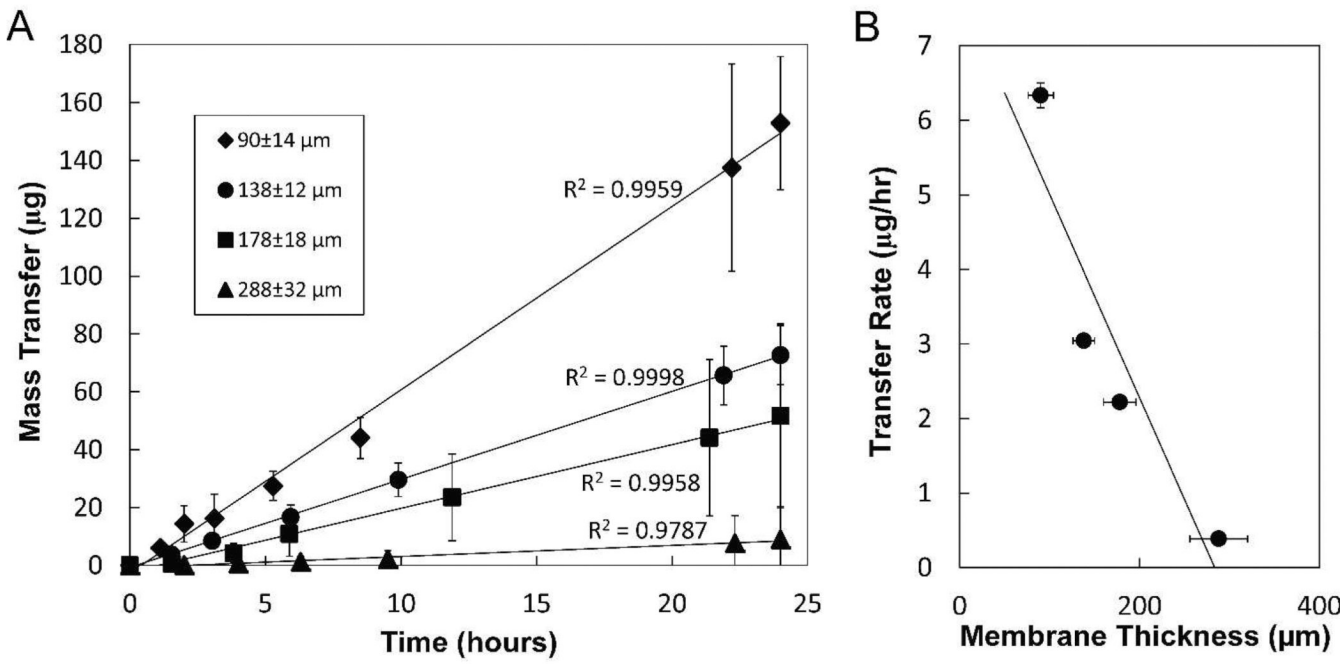

Figure 3. Membrane thickness regulates sodium fluorescein flux

(A) Mass transfer of sodium fluorescein as a function of "on" triggering time for membranes with different thicknesses. (B) Rate of mass transfer as a function of membrane thickness for data represented in panel A. All data are for sodium fluorescein flux, 25 wt% NG-37 membranes. Data are means ± SD; for each set, n = 6.

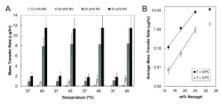

Figure 4. Nanogel content of membranes regulates membrane flux

(A) Repeated "on" and "off" cycles with temperature triggering at ca. 12-hour time intervals. (B) Average mass transfer rates of all cycles represented in panel A. Note the logarithmic scale. Data are for sodium fluorescein flux, NG-37 membranes. Data are means ± SDs; n =5, 4, 6, 6 for 12, 18, 25 and 32 wt% membranes, respectively.

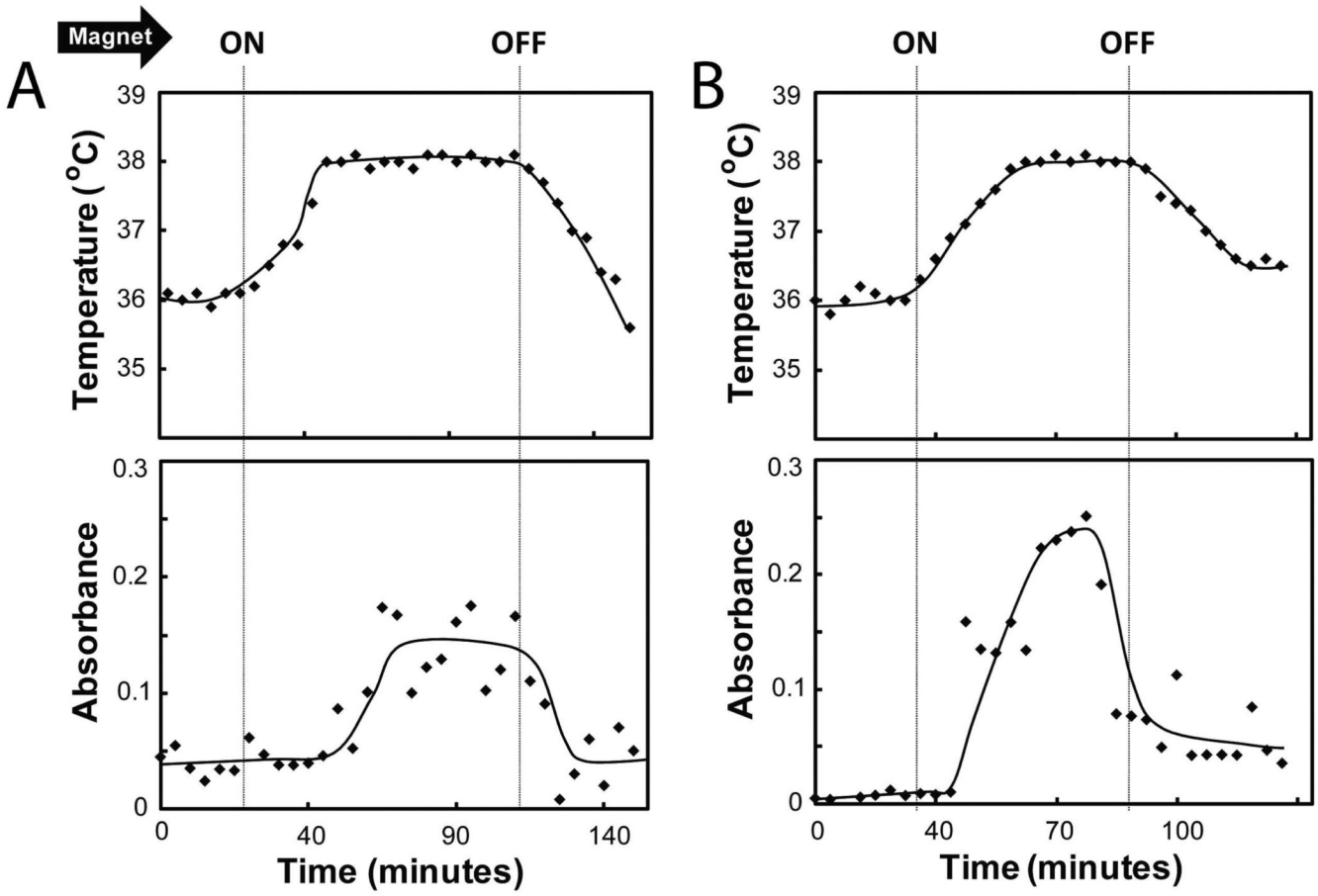

Figure 5. Magnetic triggering of membranes

Devices filled with sodium fluorescein and capped with membranes were turned “on” by an oscillating magnetic field (220–260 kHz, 0–20 mT). We separately measured devices containing (A) 23 wt% NG-37 or (B) 28 wt% NG-37 membranes.

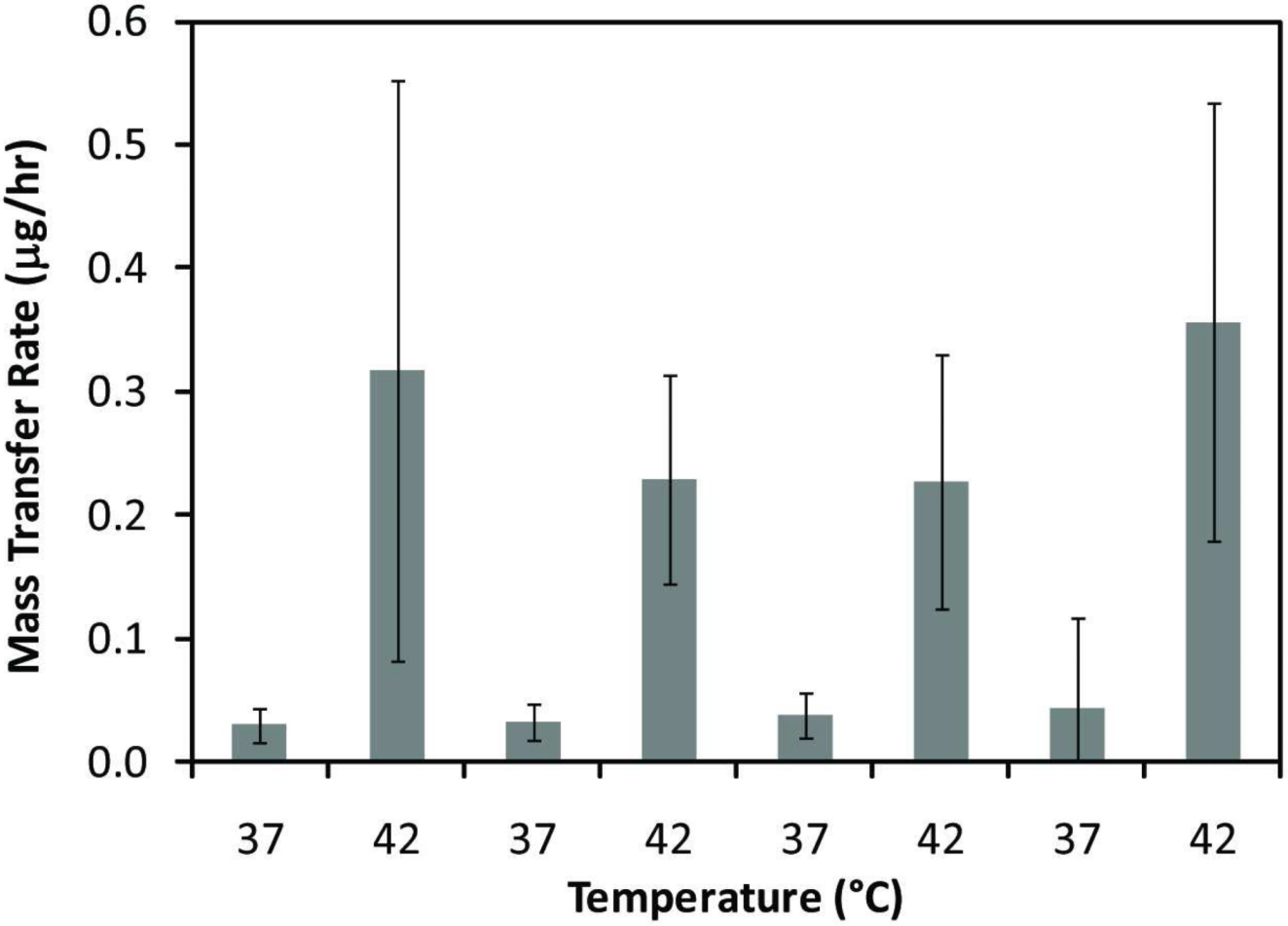

Figure 6. Membranes can deliver large molecular weight molecules

Mass rate of drug release through nanogel-filled magnetic membranes as a function of temperature (fluorescein-labelled dextran (40kDa molecular weight), 1.25mg/mL source solution, 25 wt% NG-37 membrane, thermal stimulus, ca. 4-hour time intervals. Data are means ± SDs; n=5.

Table 1

Composition and thermal phase transition temperatures of four nanogels synthesized for membrane testing. Each membrane also contains 5 mol% N,N-methylenebisacrylamide crosslinker.

nanogel [a]	n-isopropylacrylamide (NIPAm, mol%)	n-isopropylmethacrylamide (NIPMAm, mol%)	acrylamide (AAm, mol%)	transition temperature (°C)
NG-32	100	0	0	32
NG-37	54	35	11	37
NG-42	35	58	7	42
NG-46	34	55	11	46

[a] The nanogel number refers to the transition temperature (right column).

Table 2

Volume change (% volume change) on deswelling for the four nanogels synthesized for membrane testing

nanogel	% volume change on deswelling
NG-32	−95.1 ± 2.9
NG-37	−98.0 ± 2.5
NG-42	−95.2 ± 2.2
NG-46	−94.8 ± 2.8